NEURO-FUZZY MODELING AND MPPT CONTROL OF PHOTOVOLTAIC ARRAYS FEEDING VSI INDUCTION MOTOR DRIVES

Mohamed A. AWADALLAH
Department of Electrical Power and Machines
University of Zagazig
Zagazig 44111, Egypt
awadalla@ksu.edu
(On leave to YIC, Saudi Arabia)

Fawzan SALEM
P.E. and Energy Conversion Department,
Electronics Research Institute, Egypt
Cairo 12622, Egypt
fawzan@lycos.com
(On leave to YIC, Saudi Arabia)

Abstract: *The paper presents a maximum power point tracking (MPPT) approach and a modeling technique for photovoltaic (PV) arrays feeding voltage-source inverter (VSI) induction motor driving a water pump load. The proposed methodology is based on adaptive neuro-fuzzy inference systems (ANFIS) employed to obtain the chopper duty ratio which guarantees maximum power operation, and to model the PV array. A pilot module of the array is periodically tested to estimate the solar irradiation and cell temperature to avoid the high cost and technical difficulties of direct measurement. Results show that maximum power operation was maintained under different loading and environmental conditions with acceptable performance of the induction motor drive.*

Keywords: *Photovoltaic arrays, maximum power point tracking, neuro-fuzzy systems, induction motor drives.*

1. Introduction

The past few decades are characterized by the growth in energy demand along with the anticipation of reduction or even extinction of conventional fuel sources. The concerns about environmental preservation have also increased. Accordingly, research and development endeavors on alternative energy sources – which are clean, renewable, and with little environmental impact – have been recently intensified. Solar energy, as a renewable energy source, is a good choice for electric power generation due to its availability and cleanliness. The solar energy is directly converted to electrical energy by solar photovoltaic (PV) cells, which could be arranged in modules or arrays. However, PV arrays still have relatively low conversion efficiency and relatively high initial cost. Moreover, PV arrays are attributed by nonlinear current-voltage (I-V) curves, and for each curve there is a single point at which the array gives maximum power. Since the I-V curves vary with the unpredictable change in solar irradiation and cell temperature, operation at maximum power point (MPP) of the solar array becomes a crucial task in PV systems [1].

Several maximum power point tracking (MPPT) techniques are currently available in the literature. Such methods vary in complexity, cost, range of effectiveness, required sensors, convergence speed, hardware implementation, and various other aspects [2]. Some of these methods are perturb and observe [3], incremental conductance [4], fractional open-circuit voltage [5], fractional short-circuit current [6], look-up table [7], array reconfiguration [8], IMPP and VMPP computation [9], best fixed voltage [10], variable inductor MPPT [11], and variable step-size incremental resistance [12]. Due to the nonlinearity of PV systems, artificial intelligence paradigms such as artificial neural networks [13], fuzzy logic control [14], and particle swarm optimization [15] could be effectively employed in order to enhance system performance.

In 1993 [16], Jang coined the term ANFIS which stands for Adaptive Network-based Fuzzy Inference Systems, or semantically equivalently, Adaptive Neuro-Fuzzy Inference Systems. ANFIS is an intelligent regime comprising an adaptive network performing the function of a Sugeno-type fuzzy model [17] and [18]. Optimization algorithms employed through adaptive networks make the system performance similar, with minimal error, to a

targeted training data set. ANFIS combines the optimization strength of adaptive networks with the ability of fuzzy systems to handle vague situations and process uncertain data. Such attribute enabled ANFIS to find many immediate engineering applications including, but not limited to, decision making, problem solving, pattern recognition, nonlinear mapping, system modeling, and adaptive control.

In the area of solar energy research, ANFIS was successfully employed to extract the MPP of PV modules [19] – [21]. Most of the research is centered on the principle of adjusting the voltage of the solar PV module by changing the duty ratio of DC-DC chopper circuits. The duty ratio is controlled for a given solar irradiation and cell temperature condition by a closed-loop scheme. Therefore, measuring the continuously changing environmental conditions becomes inevitable as well as the usage of control system components, which increases the overall system cost. In addition to application to system modeling [22] – [24], ANFIS was also employed to estimate the chopper duty ratio directly from solar irradiation and module temperature [20]. Up to the best of the authors' knowledge, there is no research work on hand that could utilize ANFIS in a MPPT application to eliminate the need to measure solar radiation and temperature.

The present paper introduces an ANFIS-based maximum power point tracking (MPPT) scheme for a photovoltaic (PV) array feeding voltage source-inverter (VSI) induction motor driving a water pump load. Since maximum power operation is dependent on the environmental conditions of the PV array, a MPPT ANFIS is primarily developed to obtain the chopper duty ratio for MPP from the solar irradiation and cell temperature. Nevertheless, due to the expensive sensors and technical difficulties of direct measurement, a pilot module of the PV array is used for periodical testing of the open-circuit voltage (V_{oc}) and short-circuit current (I_{sc}). The measured V_{oc} and I_{sc} are used to estimate the solar irradiation and cell temperature via two other independent ANFIS, which can model the highly nonlinear behavior of the module. Thus, the chopper duty ratio for MPP is estimated over two stages: first is to assess the solar irradiation and cell temperature from pilot module testing, and second is to deduce the duty ratio from the estimated environmental conditions. Finally, the functions developed so far are combined in one ANFIS, represented by the dashed box of Fig. 1, inferring the duty ratio directly from pilot module testing. Results show acceptable performance of all developed ANFIS as well as the induction motor drive representing the load of the system. The most distinct feature of the proposed method is the elimination of the need to measure irradiation and temperature. The arbitrarily set frequency of pilot module testing is also a plus, which enables the system to cope with the rapidly changing environmental conditions.

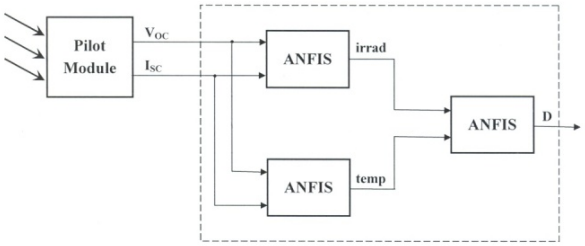

Fig. 1: Proposed ANFIS structure

2. Problem Formulation

The system, Fig. 2, consists of a PV array feeding a buck chopper, whose duty ratio is controlled to maintain maximum power operation of the PV. The constant DC output voltage of the chopper feeds a three-phase inverter switched in open loop by the standard sinusoidal pulse-width modulation (SPWM) algorithm. The battery at the DC link helps maintain the chopper output voltage constant such that controlling the duty ratio would force the PV voltage to the MPP value. The battery also helps regulate the power flow from the PV panel to the motor drive. It can store or compensate the difference between the PV output and load power. The fixed voltage and frequency output AC voltage of the inverter feeds three-phase induction motor driving a water pump load. The maximum power point of the PV is dependent on the environmental conditions represented by solar irradiation and cell temperature. Such conditions determine the chopper duty ratio required to run the PV at maximum power and obtain constant output DC voltage.

The duty ratio of the chopper for MPP operation is directly related to solar irradiation and cell temperature. Therefore, a two-input one-output ANFIS is developed to mimic such relationship. However, the Pyranometer used to measure solar irradiation is known to be expensive and sensitive to changes of the operating conditions. Meanwhile, measurement of cell temperature is not technically straightforward as cell temperature is different from

ambient temperature due to cell-loss accumulated heat. Empirical formulae could be used to estimate cell temperature from the easily measured ambient temperature; however, results are usually inaccurate. Due to such obstacles of direct measurement, an innovative technique is proposed to deduce the irradiation and temperature from a pilot module of the PV array. The pilot module is periodically tested to measure its open-circuit voltage and short-circuit current. Then, two ANFIS, both having two inputs and one output, are developed to obtain the solar irradiation and cell temperature from the pilot module measurements. Thus, the need for direct measurement of environmental conditions is eliminated.

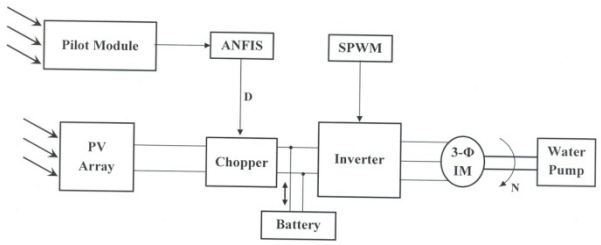

Fig. 2: System structure

The next step is to combine the three functions performed by ANFIS – as indicated by the dashed box of Fig. 1 – into one ANFIS. Therefore, a two-input one-output ANFIS is developed to estimate the chopper duty ratio for MPPT directly from V_{oc} and I_{sc} measured from the pilot module. A distinct feature of the proposed technique is that repetitive testing of the pilot module could be performed as frequent as needed, which guarantees that the system can cope with fast changing environmental conditions.

2.1 Mathematical Model of the PV Array

A solar cell can be modeled with a current source in parallel to a diode, a shunt resistor to represent ground leakage, and a series resistor to account for power loss associated with cell current, Fig. 3(a). The cell current is expressed as.

$$I_c = I_{ph} - I_{os}\left[e^{\frac{q}{AKT}(V_c + I_c R_s)} - 1\right] - \frac{(V_c + I_c R_s)}{R_{sh}} \quad (1)$$

Where:
I_c = Cell current, A,
I_{ph} = Light-generated current, or photocurrent, A,
I_{os} = Reverse saturation current of the diode, A,
q = Electron charge, C,
A = Ideality factor of the diode,
K = Boltzmann constant, J/^{o}K,
T = Cell Temperature, ^{o}K,
V_c = Cell voltage, V,
R_s = Series resistance, Ohm, and
R_{sh} = Shunt resistance, Ohm.

The photocurrent is dependent on the solar irradiation and cell temperature, and is given as.

$$I_{ph} = \lambda\left[I_{sc} + k_i\left(T - T_r\right)\right] \quad (2)$$

Where:

λ = Solar irradiation (as a ratio of 1000 W/m^2), suns,
I_{sc} = Cell S.C. current at a 25°C and 1000 W/m^2, A,
k_i = S.C. current temperature coefficient, A/^{o}K,
T and T_r = Actual and reference temperature, ^{o}K.

On the other hand, the reverse saturation current varies with temperature, and could be expressed as.

$$I_{os} = I_{or}\left(\frac{T}{T_r}\right)^3 e^{\frac{qE_g}{AK}\left(\frac{1}{T_r} - \frac{1}{T}\right)} \quad (3)$$

Where:
I_{or} = Reverse saturation current at reference temperature and irradiation, A,
T and T_r = Actual and reference temperature, ^{o}K,
E_g = Band-gap energy of the semiconductor used in the cell, J/C.

The shunt resistance, R_{sh}, is inversely related with shunt leakage current to the ground. In general, the PV efficiency is insensitive to variation in such resistance, which can be assumed to approach infinity with no leakage current to ground. On the other hand, a small variation in R_s will significantly affect the PV output power. Therefore, the shunt resistance is usually neglected in the cell equivalent circuit.

Since a typical PV cell produces less than 2W at 0.5V approximately, the cells must be connected in series-parallel configuration on a module to produce enough high power. A PV array is a group of several modules which are electrically connected in series and parallel to generate the required current and voltage. The equivalent circuit of a solar array with N_s and N_p series and parallel cells is shown in Fig. 3(b). The terminal equation of the array current becomes as follows.

$$I = N_p I_{ph} - N_p I_{os}\left[e^{\frac{q}{AKT}\left(\frac{V}{N_s} + \frac{IR_s}{N_p}\right)} - 1\right] - \frac{1}{R_{sh}}\left[\frac{N_p}{N_s}V + IR_s\right] \quad (4)$$

In fact, the PV efficiency is sensitive to small change in the series resistance, but insensitive to variation in the shunt resistance. In most commercial products, PV cells are generally connected in series to form a PV module in order to obtain adequate operating voltage. Modules are then arranged in series-parallel structure to form an array and achieve the desired output power.

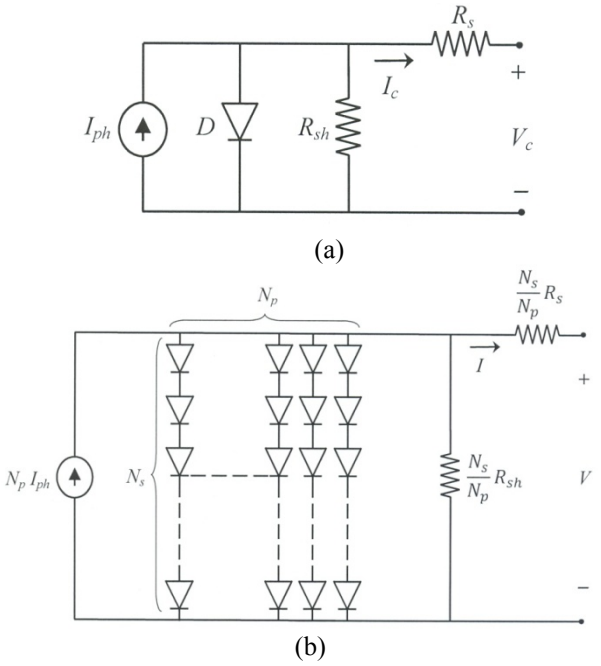

Fig. 3: Equivalent circuits: (a) PV cell, (b) PV array.

The above equations are directly employed to obtain the current-voltage characteristics of the PV array. The maximum power point is signified by certain array voltage and current, and is determined by the solar irradiation and cell temperature. Forcing the array voltage to the value required for maximum power, as the environmental conditions change, guarantees MPPT. If the load-side voltage of the chopper is to be maintained constant, the duty ratio should be continuously varied in order to assure maximum power operation. Such task is performed via ANFIS in the present work.

3. Adaptive Neuro-Fuzzy Inference Systems (ANFIS)

ANFIS refers, in general, to an adaptive network which performs the function of a fuzzy inference system [16] – [18]. The most commonly used fuzzy system in ANFIS architectures is the Sugeno model since it is less computationally exhaustive and more transparent than other models, especially when processed by machines. In the premise part, the Sugeno model is not different from other fuzzy systems, of which the most famous is the Mamdani model. A consequent membership function (MF) of the Sugeno model could be any arbitrary parameterized function of the crisp inputs, most likely a polynomial. Zero and first order polynomials are used as consequent MF in constant and linear Sugeno models, respectively. In addition, the defuzzification process in Sugeno fuzzy models is a simple weighted average calculation. The fuzzy space is divided via grid partitioning according to the number of antecedent MF, and each fuzzy region is covered with a fuzzy rule. On the other hand, each fixed and adaptive node of the network performs one function or sub-function of the Sugeno model, as shown in Fig. 4, such that the overall performance of the network is functionally the same as that of the fuzzy model.

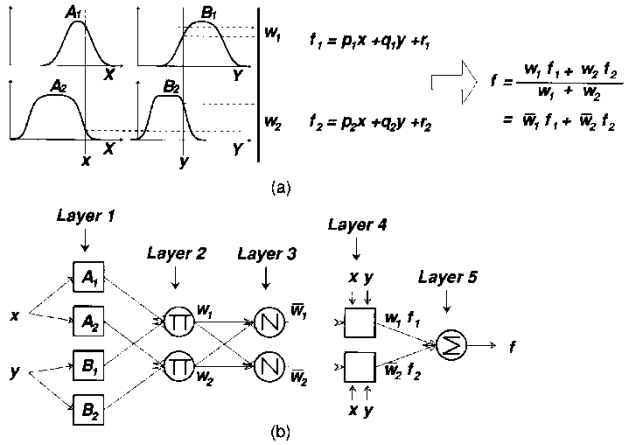

Fig. 4: (a) Two-input, one-output, two-rule Sugeno model, (b) equivalent ANFIS structure.

The adaptive network employs an optimization algorithm in order to modify the parameters of the fuzzy inference system. The adaptation process aims at obtaining a set of parameters at which an error measure between the actual performance of the fuzzy inference system and a targeted set of training data is minimized. Parameters of the consequent MF are linear as long as zero or first order polynomials are used; meanwhile, parameters of the antecedent MF are nonlinear.

Thus, classical optimization techniques, such as back propagation, could be used as well as hybrid algorithms. The total number of ANFIS modifiable parameters is a crucial factor of the computational effort required before the adaptation process is completed. Therefore, antecedent Gaussian MF, which is defined through two parameters only, is more preferable than other forms of MF, which

require three or more parameters. ANFIS combines the advantages of fuzzy systems and adaptive networks in one hybrid intelligent paradigm. The flexibility and subjectivity of fuzzy inference systems, when added to the adaptation potential of adaptive networks, give ANFIS its remarkable power of modeling, learning, nonlinear mapping, and pattern recognition.

4. Results

The task of MPPT in the system of Fig. 2 is accomplished through ANFIS. Ultimately, the chopper duty ratio is deduced from the measurements of open-circuit voltage and short-circuit current of the pilot module. Then, the system is modeled under maximum power operation to check for acceptable performance of the induction motor drive and its load.

4.1 ANFIS development

Operation of the PV array varies with changes of the solar irradiation and cell temperature; accordingly, MPP is reliant on such independent variables of the system. As a first thought, the chopper duty ratio is estimated from solar irradiation and cell temperature via ANFIS. The training data are obtained by solving the mathematical model of the PV array – Equations (1) through (4) – at different environmental conditions. The solar irradiation is changed from 300 to 1000 by a step of 10 W/m^2, and the cell temperature is varied from 290 to 325 by a step of 5 ^{o}K, resulting in a training data set of 568 points. The chopper duty ratio for maximum power is computed at each point to represent the corresponding ANFIS output. A two-input one-output ANFIS is designed with Gaussian antecedent membership function (MF), and first-order polynomial consequent MF. With three MF per input, the mean square error (MSE) of the training data did not stagnate even after 1500 training epochs. However, with four, five, and seven MF per input, MSE stagnated at 0.0001296, 0.0001031, and 8.44×10^{-5} after 64, 4, and 4 training epochs, respectively. It should be mentioned that all ANFIS of the present work are developed using the Fuzzy Logic Toolbox of Matlab 7.8, where the hybrid training algorithm is always used for training.

A fifty-point testing data set is similarly derived from the mathematical model at randomly selected conditions. It should be highlighted that testing data are not subset of the training data; moreover, some points are outside the range of training data. The MSE of the testing data is 0.0028, 0.009, and 0.0083 for the four, five, and seven MF per input cases, respectively. In compromise between system size and accuracy, the four MF per input ANFIS is chosen. Table 1 shows sample results of ANFIS testing.

The results of another more systematic method of ANFIS testing are shown in Fig. 5. Typical variations of solar irradiation and temperature of a summer day are shown from 6 am to 6 pm. Both curves are normal distributions with maximum points occurring at noon for irradiation, and at 2 pm for temperature. The bottom plot of the figure shows the chopper duty ratio where the solid curve indicates the required values and the dotted one signifies ANFIS output. The plot shows that ANFIS output is almost identical to the required duty ratio at MPP. However, there is a slight difference at both tails of the plot because the actual irradiation values are outside the training range of ANFIS. Nevertheless, such difference is still acceptable.

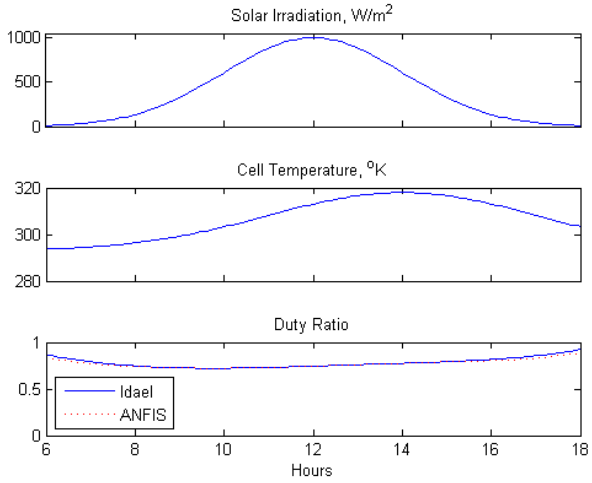

Fig. 5: Results of ANFIS testing during a typical summer day.

The above ANFIS requires solar irradiation and cell temperature to be continuously measured in order to estimate the chopper duty ratio. Measuring such quantities is known to be expensive and troublesome. The Pyranometer used to measure solar irradiation is a costly device. In addition, cell temperature normally differs from ambient temperature due to internal losses associated with load and leakage currents. Even when some empirical formulae are used to estimate cell temperature from ambient temperature, results are

usually inaccurate. Hence, there is a solid motivation to deduce solar irradiation and cell temperature in order to avoid measuring them. A pilot module of the PV panel could be used solely for such purpose. The open-circuit voltage (V_{oc}) and short-circuit current (I_{sc}) of the pilot module are periodically measured to estimate solar irradiation and cell temperature using ANFIS agents which would model the nonlinear PV behavior. Two separate ANFIS are developed; both have V_{oc} and I_{sc} as inputs, while one outputs solar irradiation and the other outputs cell temperature. It should be emphasized that conceptually, a two-input two-output ANFIS could have performed the task equivalently well. However, it is a limitation of the Fuzzy Logic Toolbox of Matlab to have only one output per ANFIS.

To estimate solar irradiation, a two-input one-output ANFIS is developed with Gaussian antecedent MF and linear consequent MF. The previous 568 operating points are re-oriented to compose the training data of the present ANFIS. When the antecedent MF are three, four and five, the training data error stabilized at 0.0095, 0.001, and 0.0117 after 76, 25, and 13 training epochs, respectively. When ANFIS is tested at the same 50 randomly selected points, MSE of testing data becomes 0.0436, 0.3025, and 15.6617 for three, four, and five MF per input, respectively.

A similar ANFIS is designed to infer cell temperature from the pilot module measurements. With three, four, and five Gaussian MF per input, and 68, 31, and 14 training epochs, the MSE error of the training data reached a minimum of 0.0295, 0.0297, and 0.0376, respectively. Results of testing at the same 50 operating conditions show a MSE of 0.5549, 2.5412, and 48.1551 for three, four, and five MF per input, respectively. Obviously, the three antecedent MF systems gave the best performance in both cases. Sample testing results for irradiation and temperature estimation systems are shown in Table 2.

The two modeling ANFIS are also tested using the typical daily variations of environmental conditions, Fig 6. The two top plots of Fig. 6 represent the day-time variations of V_{oc} and I_{sc} of the pilot module due to the change in solar irradiation and cell temperature.

The two bottom plots show ANFIS performance in detecting irradiation and temperature, where the solid curves indicate the actual values, while the dotted curves signify ANFIS output. The plots denote excellent matching between actual and predicted values except for the first and last two hours of the day on the temperature plot only. The reason again is that the actual values of irradiation during such periods are outside the training range of ANFIS. Yet, ANFIS output is still of acceptable accuracy as the percentage error is 8.715% and 8.797% at 6 am and 6 pm, respectively. It should be emphasized that ANFIS performance could be improved if the training data range is extended to include small irradiation values, which are likely to be at the beginning and ending hours of the day.

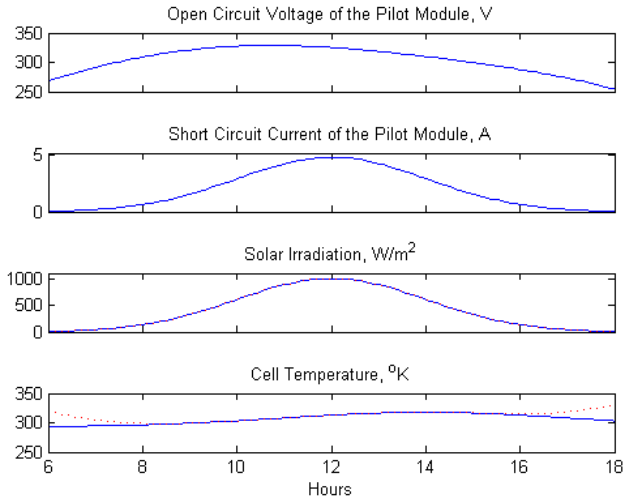

Fig. 6: Results of modeling ANFIS testing during a typical summer day.

The last, and concluding, step of ANFIS development is to design a system that deduces the chopper duty ratio directly from pilot module testing. Accordingly, a two-input one-output ANFIS is designed with Gaussian and linear antecedent and consequent MF, respectively. Inputs are V_{oc} and I_{sc} obtained from pilot module testing, while the output is straightforwardly the chopper duty ratio. The same 568 operating points are used for training, and the same 50 random points are used for testing. The training MSE becomes fixed at 0.00012, 0.00013, and 0.00014 after 129, 4, and 2 epochs with 3, 4, and 5 MF per input, respectively. However, MSE based on testing data of the 3, 4, and 5 antecedent MF systems is 0.0036, 0.0089, and 0.1227, respectively. Evidently, the 3 MF per input ANFIS outperforms the other two cases of 4 and 5 MF per input. Table 2 shows sample testing points.

Table 1: Results[1] of ANFIS testing.

Case	Inputs		Output (Duty Ratio)		Error	
	Irradiation, W/m^2	Temperature, ^{o}K	Actual	Estimated	Absolute	Percentage
1	229	283	0.6833	0.6808	– 0.0025	– 0.3687
2	484	296	0.7046	0.7044	– 0.0002	– 0.0284
3	994	309	0.7314	0.7313	– 0.0001	– 0.0137
4	739	322	0.7856	0.7857	0.0001	0.0127
5	229	335	0.8943	0.8841	– 0.0102	– 1.1406

[1]Inputs are solar irradiation and cell temperature

Table 2: Results[2] of ANFIS testing.

Case	Inputs		Output (Irradiation, W/m^2)		Error	
	V_{oc}, V	I_{sc}, A	Actual	Estimated	Absolute	Percentage
1	335.1	1.0920	229	229.088	0.088	0.0384
2	360.1	4.7399	994	993.934	– 0.066	– 0.0066
3	308.3	1.5145	314	314.004	0.004	0.0013
4	319.4	2.7443	569	568.998	– 0.002	– 0.0004
5	284.5	2.3608	484	484.023	0.023	0.0048
Case	Inputs		Output (Temperature, ^{o}K)		Error	
	V_{oc}, V	I_{sc}, A	Actual	Estimated	Absolute	Percentage
1	340.5	1.4973	283	283.181	0.181	0.064
2	318.8	1.0982	296	296.486	0.486	0.1642
3	322.0	3.1543	309	308.947	– 0.053	– 0.0172
4	312.7	4.4090	322	322.014	0.014	0.0043
5	287.8	2.7754	335	334.6	– 0.4	– 0.1194
Case	Inputs		Output (Duty Ratio)		Error	
	V_{oc}, V	I_{sc}, A	Actual	Estimated	Absolute	Percentage
1	353	3.1186	0.6591	0.6580	– 0.0011	– 0.1669
2	302.5	1.1045	0.7754	0.7752	– 0.0002	– 0.0258
3	358.6	4.3346	0.654	0.6533	– 0.0007	– 0.107
4	275.8	1.5316	0.8767	0.8722	– 0.0045	– 0.5133
5	286	1.1107	0.8308	0.8310	0.0002	0.0241

[2] Inputs are V_{oc} and I_{sc} of the pilot module

Testing results show that ANFIS could estimate the targeted output very precisely. One distinct contribution of the present work is the elimination of the need to measure solar irradiation and cell temperature in order to estimate the chopper duty ratio for MPPT. Rather, two inexpensive- and easily-measured quantities, i.e. V_{oc} and I_{sc} of the pilot module, are employed. Another advantage of the proposed technique is that the pilot module could be arbitrarily frequently tested in order to cope with rapidly varying environmental conditions.

4.2 Drive performance

The DC output voltage of the buck chopper feeds a three-phase inverter switched in open loop operation by the standard SPWM technique. The fundamental frequency of the output waveform is 60 Hz, while the frequency ratio and modulation index

of the SPWM algorithm are 18 and 0.8, respectively. The fixed-voltage fixed-frequency output of the inverter feeds a three-phase induction motor whose parameters are given in Appendix I. Water pump is modeled as a linear speed-dependent torque [20] by

(5)

A Simulink model is used to investigate the drive performance under different operating conditions. The drive performance is always acceptable as indicated by the sample case of Fig. 7, which shows the motor line voltage, current, torque and speed at 850 W/m^2 irradiation and 295 ^{o}K temperature. At such condition, the required output voltage, current, and power of the PV panel for MPP are 270.5 V, 3.801 A, and 1028 W, respectively. The proposed MPPT technique yields output voltage, current, and power of 278.4 V, 3.822 A, and 1064 W, respectively. The error of the PV output power in this case is +3.5%. The average developed torque is 6.362 Nm, the peak-to-peak ripple torque is 1.64, while the shaft speed is 1477 RPM.

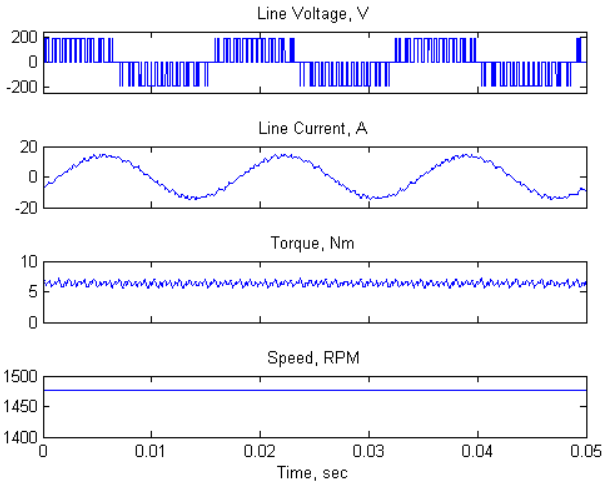

Fig. 7: Motor performance characteristics at 850 W/m^2 and 295 ^{o}K.

The frequency spectra of the motor line voltage and current are plotted in Fig. 8 up to the 49th harmonic. Beyond the fundamental component, only four voltage harmonics are of significant values. Such harmonics are the 16th, 20th, 35th, and 37th, of which the 35th has the maximum relative value of 39.84% of the fundamental. On the current spectrum, all harmonics but the fundamental are almost negligible. However, the maximum current harmonic is the 16th, which represents 4.24% of the fundamental component. The performance of the motor drive is investigated at other operating conditions of the system, and is found always acceptable.

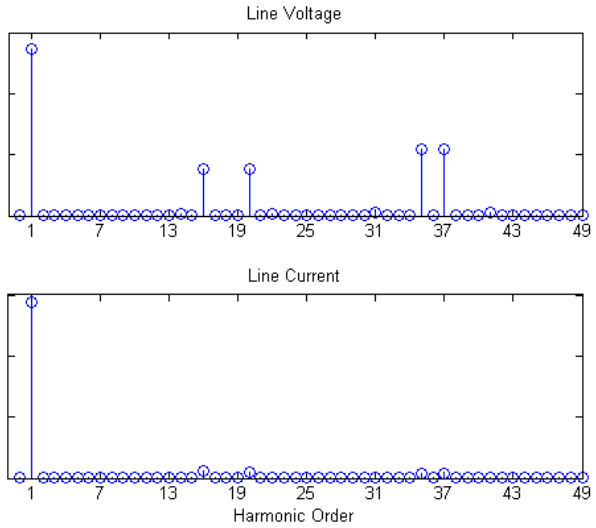

Fig. 8: Frequency spectra of the motor line voltage and current at 850 W/m^2 and 295 ^{o}K.

5. Conclusions

The paper presents an ANFIS-based methodology for MPPT in PV arrays. The system consists of a PV array comprising 576 solar cells connected in series. A buck chopper follows the PV array in order to convert its varying MPP voltage into a fixed voltage feeding a three-phase inverter. The inverter is controlled in open-loop by SPWM switching logic to feed a three-phase induction motor driving a water pump. A battery is connected across the DC link to fix the chopper output voltage and compensate for the energy difference between the PV panel and load. Firstly, ANFIS is used to estimate the chopper duty ratio for MPP operation from solar irradiation and cell temperature. Then, a pilot module of the PV array is used to periodically check its open circuit voltage and short circuit current. ANFIS is applied to model the PV behavior and infer the solar irradiation and cell temperature from the pilot module testing. Lastly, one ANFIS is developed to deduce the chopper duty ratio for MPPT directly from pilot module testing. Results show excellent ANFIS performance whether in PV array modeling or in MPPT; operation of the induction motor drive is also investigated and found acceptable under different environmental conditions.

The contribution of the present work stems from the elimination of the need to measure irradiation and temperature which are costly and technically troublesome when directly measured. In addition, the pilot module could be arbitrarily frequently tested to cope with rapidly changing environmental conditions.

References

1. Tse, K., Billy, M., Henry S., and Ron Hui, S.: *A Comparative study of maximum-power-point trackers for photovoltaic panels using switching-frequency modulation scheme.* In: IEEE Transactions on Industrial Electronics, Vol. 51, No. 2, April 2004, p. 410-418.
2. Walker, S., Sooriyaarachchi, N., Liyanage, N., and Abeynayake, P.: *Comparative analysis of speed of convergence of MPPT techniques*. In: 6th International Conference on Industrial and Information Systems, ICIIS, Sri Lanka, Aug. 16-19, 2011, p. 522-526.
3. Piegari, L. and Rizzo, R.: *Adaptive perturb and observe algorithm for photovoltaic maximum power point tracking.* In IET Renewable Power Generation, Vol. 4, No. 4, 2010, p. 317-328.
4. Eftichios, K., Kostas, K., and Nicholas, C.: *Development of a microcontroller-based photovoltaic maximum power point tracking control system*. In: IEEE Transactions on Power Electronics, Vol. 16, No. 1, January 2001, p. 46-54.
5. Jawad, A.: *A fractional open circuit voltage based maximum power point tracker for photovoltaic arrays*. In: 2nd International Conference on Software Technology and Engineering (ICSTE), Vol. 1, 2010, p. 247-250.
6. Esram, T. and Chapman, P.: *Comparison of photovoltaic array maximum power point tracking techniques*. In: IEEE Transactions on Energy Conversion, Vol. 22, No. 2, June 2007, p. 439-449.
7. Tarik Duru, H.: *A maximum power tracking algorithm based on $I_{mpp} = f(P_{max})$ function for matching passive and active loads to a photovoltaic generator.* In: Solar Energy, Vol. 80, No. 7, 2005, p. 812-822.
8. El-Shibini, M. and Rakha, H.: *Maximum power point tracking technique*. In: Proc. Integrating Research, Ind. Educ. Energy Commun. Eng. Electrotechnical Conf., 1989, p. 21-24.
9. Takashima, T., Tanaka, T., Amano, M., and Ando, Y.: *Maximum output control of photovoltaic (PV) array*. In: Proc. 35th Intersociety Energy Convers. Eng. Conf. Exhib., 2000, p. 380-383.
10. Carvalho, P., Pontes, R., Oliveira, D., Riffel, D., Oliveira, R., and Mesquita, S.: *Control method of a photovoltaic powered reverse osmosis plant without batteries based on maximum power point tracking*. In: Proc. IEEE/PES Transmiss. Distrib. Conf. Expo.: Latin America, 2004, p. 137-142.
11. Zhang, L., Hurley, W., and Wolfle, W.: *A new approach to achieve maximum power point tracking for PV system with a variable inductor*. In: 2nd IEEE International Symposium on Power Electronics for Distributed Generation Systems, 2010, p. 948-952.
12. Mei, Q., Shan, M., Liu, L., and Guerrero, J.: *A novel improved variable step-size incremental resistance MPPT method for PV systems*. In: IEEE Transactions on Industrial Electronics, Vol. 58, No. 6, 2010, p. 2427-2434.
13. Abdessamia, E., Dhafer, M., and Abdelkader M.: *A maximum power point tracking method based on artificial neural network for A PV system*. In: International Journal of Advances in Engineering and Technology, Vol. 5, No. 1, November 2012, p. 130-140.
14. Theodoros, L., Yiannis, S., and Athanassios, D.: *New maximum power point tracker for PV arrays using fuzzy controller in close cooperation with fuzzy cognitive networks*. In: IEEE Transactions on Energy Conversion, Vol. 21, No. 3, September 2006, p. 793-803.
15. Hu, Y., Liu, J., and Liu, B.: *A MPPT control method of PV system based on fuzzy logic and particle swarm optimization.* In: Second International Conference on Intelligent System Design and Engineering Application, 2011, p. 73-75.
16. Jang, J.-S.: *ANFIS: Adaptive-network-based fuzzy inference system*. In: IEEE Transactions on Systems, Man, and Cybernetics, Vol. 23, No. 3, 1993, p. 665-685.
17. Jang, J.-S., Sun, C.-T., and Mizutani, E.: *Neuro-Fuzzy and Soft Computing – A Computational Approach to Learning and Machine Intelligence*. Prentice-Hall, 1997.
18. Cox, E.: *Fuzzy fundamentals*. In: IEEE Spectrum, Vol. 29, No. 10, 1992, p. 58-61.
19. Iqbali, A., Abu-Rub, H., and Ahmed, Sk.: *Adaptive neuro-fuzzy inference system based maximum power point tracking of a solar PV module.* In: IEEE International Energy Conference, 2010, p. 51-56.
20. Farhat, M. and Lassâad, S.: *Advanced ANFIS-MPPT control algorithm for sunshine photovoltaic pumping systems.* In: 1st International Conference on Renewable Energies and Vehicular Technology, 2012, p. 167-172.
21. Haitham, A., Atif I., Moin A., Fang, Z., Yuan Li, and Ge, B.: *Quasi-Z-source inverter-based photovoltaic generation system with maximum power tracking control using ANFIS.* In: IEEE Transactions on Sustainable Energy, Vol. 4, No. 1, January 2013, p. 11-20.
22. Mellit, A. and Kalogirou, S. A.: *Neuro-fuzzy based modeling for photovoltaic power supply system*. In: First International Power and Energy Conference, 2006, p. 88-93.
23. Durgadevi, A., Arulselvi, S., and Natarajan, S. P.: *Photovoltaic modeling and its characteristics*. In: International Conference on Emerging Trends in Electrical and Computer Technology, 2011, p. 469-475.
24. Mellit, A.: *Artificial intelligence based-modeling for sizing of a stand-alone photovoltaic power system: Proposition for a new model using neuro-fuzzy system (ANFIS)*. In: 3rd International IEEE Conference on Intelligent Systems, 2006, p. 606-611.

Appendix I: Simulation Parameters

PV Panel	
Number of cells in series	36×16
Number of cells in parallel	1
Reference reverse saturation current	2.35×10^{-8} A
Short-circuit current temperature coefficient	0.0021 A/^{o}K
Diode ideality factor	1.21
Series resistance per cell	0.01143 Ohm
Induction Motor	
Output	3 hp
Line Voltage	220 V
Frequency	60 Hz
Poles	4
Stator Resistance	0.435 Ohm
Stator Inductance	4 mH
Rotor Resistance	0.816 Ohm
Rotor Inductance	2 mH
Mutual Inductance	69.31 mH
Inertia	0.089 kg.m^2
Pulse Width Modulation	
Output Frequency	60 Hz
Modulation Index	0.8
Frequency Ratio	18
IGBT	
Saturation V_{CE}	0.3 V
ON-State Resistance	0.01 Ohm
T_{ON}	0
T_{OFF}	0.3 μsec